

Three-dimensional Material and Geometrical Nonlinear Analysis of Adhesively Bonded Single Lap Joint

S. Narasimhan and P.C. Pandey

Indian Institute of Science, Bangalore – 560 012

ABSTRACT

The paper presents 3-D viscoplastic analysis of adhesively bonded single lap joint considering material and geometric nonlinearity. Total Lagrangian formulation is used to develop a 3-D finite element for geometric nonlinear analysis. The overall geometry of the single lap joint, the loading, and the boundary conditions has been considered, both according to the ASTM testing standards and from those adopted in earlier investigations. The constitutive relations for the adhesive are developed using a pressure-dependant (modified) von Mises yield function and Ramberg-Osgood idealisation for the experimental stress-strain curve. The adherends and adhesive layers are both modelled using 20-noded solid elements. However, observations have been made, in particular, on peel and shear stresses in the adhesive layer, which provide useful insight into the 3-D nature of the problem.

Keywords: Adhesives, bonded joints, elasto-viscoplasticity, material nonlinearity, geometric nonlinearity, peel stress, shear stress, three-dimensional behaviour, viscoplasticity

NOMENCLATURE

C	Overlap length	J'_2, J'_3	Second and third invariants of the deviatoric stress
C_{ijkl}	Constitutive tensor for elastic materials	Q	Plastic potential
E	Young's modulus	S_{ij}	Deviatoric stress tensor
F	Yield function	α	Time-stepping parameter
H	Adherend thickness	Δt	Time step length
h	Adhesive thickness	δ_{ij}	Kronecker delta
I'_1	First invariant of the general strain tensor	ε	Green's strain
I'_2	Second invariant of the general strain tensor	ε_0	Initial strain vector
J	Deformation gradient	$\varepsilon^e, \varepsilon^p$	Elastic and viscoplastic strain components
J_1	First stress invariant	γ	Fluidity parameter
L	Adherend length	λ	Ratio of compressive to tensile yield stress

- μ Shear modulus
- ν Poisson's ratio
- $\phi(F)$ Flow function
- σ Vector of second Piola-Kirchoff stress
- σ_m Mean stress
- σ_y Effective yield stress
- $\sigma_1, \sigma_2, \sigma_3$ Principal stresses
- τ_{oct} Octahedral stress

1. INTRODUCTION

Three-dimensional material and geometric nonlinear analysis of adhesively bonded single lap joint are presented. This paper focusses on the explicit formulation of the total Lagrangian method in the context of a 3-D case, and hence, the elasto-viscoplastic formulation is given briefly¹⁻¹². The formulation is restricted to only large deformation and large rotation, but small strain problems and external loading is assumed to be constant during the deformation of the structure. The isoparametric formulation of the total Lagrangian case and various terms involved are presented explicitly. The objective of this study includes the 3-D modelling of adhesively bonded single lap joint with the adhesive layer as a viscoplastic material. Observations have been made on peel and shear stress distributions in the adhesive region through parametric study and the 3-D regions in a single lap joint have been identified.

2. GEOMETRICAL NONLINEAR FORMULATION FOR 3-D CASE

2.1 Definition of Strains & Stresses

The formulation of geometric nonlinearity and the explicit form of Lagrangian formulation can be referred to in detail in Zienkiewicz¹³.

2.1.1 Deformation & Strain

Let

$$X = [x, y, z]^T$$

define the rectangular coordinates of a material

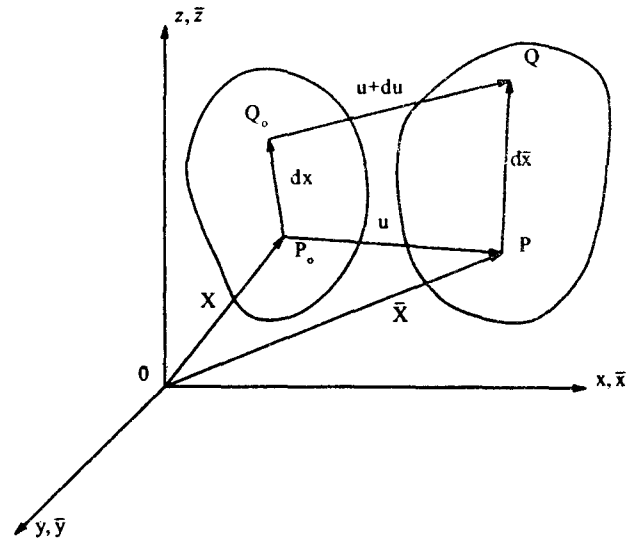


Figure 1. Motion of a body in Cartesian coordinate system

point in a body before the deformation as shown in Fig. 1. If this point is displaced by

$$u = [u, v, w]^T$$

measured relative to the fixed frame of reference, its new coordinates will become

$$\bar{X} = [\bar{x}, \bar{y}, \bar{z}]^T = X + u \tag{1}$$

Let one consider two neighbouring particles, P_0 and Q_0 on the undeformed body. These move to P and Q after deformation (Fig. 1). If the distance between P_0 and Q_0 , and P and Q are given by dS with components $d\bar{X} = [d\bar{x}, d\bar{y}, d\bar{z}]$ respectively, the relation between dX and $d\bar{X}$ is given by

$$\bar{X} = JdX \tag{2}$$

is a Jacobean matrix defining the deformed state. The change in length can be written as

$$\begin{aligned} \frac{1}{2}(d\bar{S}^2 - dS^2) &= \frac{1}{2}(d\bar{X}^T d\bar{X} - dX^T dX) \\ &= dX^T \epsilon dX = d\bar{X}^T \bar{\epsilon} d\bar{X} \end{aligned} \tag{3}$$

where

$$\varepsilon = \frac{1}{2}(J^T J - I) \quad (4)$$

is the Lagrangian definition of the strain (Green's strain) and

$$\bar{\varepsilon} = \frac{1}{2}(I - \bar{J}^T \bar{J}) \quad (5)$$

is the Eulerian definition of strain.

Substituting Eqn (1) in Eqns (4) and (5), the explicit engineering expressions for the strain components are obtained.

2.1.2 Definitions of Stresses

The natural definition of stresses $\bar{\sigma}$ is the Eulerian one referring in the usual way to the forces per unit deformed area. The forces acting on the area $d\bar{A}$ are given in the vector form as

$$d\bar{F} = \bar{\sigma} d\bar{A} \quad (6)$$

As per Hill's⁴ definition of conjugate pairs of stress and strain variables, for the Green's strain, the conjugate stress is the second Piola-Kirchoff stress σ . The equivalent force vector acting on an original undeformed area dA is given by an expression

$$dF = \sigma dA \quad (7)$$

and the actual force on the deformed area

$$d\bar{F} = JdF \quad (8)$$

But the relation between dA and $d\bar{A}$ is given by

$$d\bar{A} = |J| J^T dA \quad (9)$$

or

$$dA = |J|^{-1} J^T d\bar{A} \quad (10)$$

From Eqns (7) to (10), one has the stress transformation relation as

$$\sigma = |J| J^{-1} \bar{\sigma} J^T \quad (11)$$

which shows that the second Piola-Kirchoff stress is also a symmetric one.

2.2 Explicit Form of Lagrangian Formulation

2.2.1 Strain-displacement Relationships

The Green's strain in vector notation in the context of 3-D solids can be written using the engineering definitions as

$$\varepsilon_x = \frac{\partial u}{\partial x} + \left[\left(\frac{\partial u}{\partial x} \right)^2 + \left(\frac{\partial v}{\partial x} \right)^2 + \left(\frac{\partial w}{\partial x} \right)^2 \right] \quad (12)$$

and

$$\gamma_{xy} = \frac{\partial u}{\partial x} + \frac{\partial v}{\partial x} + \left[\frac{\partial u}{\partial x} \frac{\partial u}{\partial y} + \frac{\partial v}{\partial x} \frac{\partial v}{\partial y} + \frac{\partial w}{\partial x} \frac{\partial w}{\partial y} \right] \quad (13)$$

and so on. The strain matrix is given as

$$\varepsilon = [\varepsilon_x, \varepsilon_y, \varepsilon_z, \gamma_{xy}, \gamma_{yz}, \gamma_{zx}] = \varepsilon_0 + \varepsilon_l \quad (14)$$

where ε_0 is the usual linear, infinitesimal strain vector and ε_l is the nonlinear contribution⁸.

2.2.2 Nonlinear Equilibrium Equations

The governing nonlinear equilibrium equations will be established from the virtual work equation, in the Eulerian coordinate system. This is given by¹⁵ the integration over the deformed volume \bar{V} and the deformed area \bar{A} as

$$\int_{\bar{V}} \delta \bar{\varepsilon}^T \bar{\sigma} d\bar{V} = \int_{\bar{V}} \bar{\rho} \delta u^T q d\bar{V} + \int_{\bar{A}} \delta u^T \bar{p} d\bar{A} \quad (15)$$

in which $\bar{\rho}$ is the density in the deformed state and $\bar{\sigma}$ and $d\bar{\varepsilon}$ refer to the vector forms of the Eulerian stress and the deformation increment in the distorted coordinate \bar{X} , respectively.

Alternatively, the above equation can be written in terms of the variables referred to the original, undistorted coordinates to get

$$\int_V \delta \epsilon^T \sigma dV = \int_V \rho \delta u^T q dV + \int_A \delta u^T p dA \quad (16)$$

where σ is the second Piola-Kirchoff stress and $d\epsilon$ is the increment of Green's strain, both referred to the undeformed coordinates.

Then the relation between ρ and $\bar{\rho}$ is given by

$$\rho = \frac{\bar{\rho}}{|J|} \quad (17)$$

The tractions p defined wrt the un-deformed body are given in terms of the tractions acting over a deformed surface area¹⁶ as

$$p = \left(\frac{d\bar{A}}{dA} \right) \bar{p} \quad (18)$$

where $\bar{p} = p$, for the small strain case with $|J|=1$ and $\left(\frac{d\bar{A}}{dA} \right) = 1$

The displacement u within the element is given as a function of the n nodal displacements as

$$u = N\delta \quad (19)$$

where $\delta = [\delta_1, \delta_2, \dots, \delta_n]$ and N is a shape function matrix with $\delta_i = [u_i, v_i, w_i]$.

After substituting the above expressions for ϵ_0 and taking differentiation

$$d\epsilon_0 = B_0 d\delta; \delta_i = [u_i, v_i, w_i]^T; \delta = [\delta_1, \delta_2, \dots, \delta_n] \quad (20)$$

where B_0 is the small displacement strain matrix. Differentiation of ϵ_t yields

$$d\epsilon_t = \frac{1}{2} dA\theta + \frac{1}{2} A d\theta \quad (21)$$

which due to the structure of the matrices involved becomes

$$d\epsilon_t = A d\theta \quad (22)$$

Now, the (9 by 1) vector θ can be written as

$$\theta = Gd = [G_1 \dots G_i \dots] \begin{bmatrix} \delta_1 \\ \vdots \\ \delta_i \\ \vdots \end{bmatrix} \quad (23)$$

where

$$G_i = \begin{bmatrix} I_3 \frac{\partial N_i}{\partial x} \\ I_3 \frac{\partial N_i}{\partial y} \\ I_3 \frac{\partial N_i}{\partial z} \end{bmatrix} \quad (24)$$

and I_3 is a 3 by 3 identity matrix.

Substituting Eqn (23) into Eqn (21), one gets

$$d\epsilon_t = B_t d\delta \quad (25)$$

with

$$B_t = AG \quad (26)$$

Thus the strain displacement matrix becomes

$$B = B_0 + B_t \quad (27)$$

The total strain matrix in Eqn (14) can be written, using Eqn (23) and (27) as

$$\epsilon = \left(B_0 + \frac{1}{2} B_t \right) \delta \quad (28)$$

For the computational purpose, it is convenient to obtain B_t explicitly by multiplying the appropriate terms in Eqn (26). The expression for the 3-D analysis shall be referred¹⁵ to.

From Eqn (19), the virtual displacement is

$$du = Nd\delta \quad (29)$$

The virtual work [Eqn (16)] is now rewritten as

$$\begin{aligned} d\delta^T \int_V B^T \sigma dV \\ = d\delta^T \int_V N^T \rho q dV + d\delta^T \int_A N^T p dA \end{aligned} \quad (30)$$

Since the virtual displacements $d\delta$ are arbitrary, Eqn (30) gives the equilibrium equations in the discretised form as

$$\int_V B^T \sigma dV + f = 0 \quad (31)$$

where the vector of equivalent nodal loads f , which comprises the vectors due to the body forces f_b , applied tractions f_p , nodal forces f_n , initial stress f_{σ_0} and the initial strain f_{ϵ_0} is given by

$$f = \int_V N^T \rho q dV + \int_A N^T p dA \quad (32)$$

This is identical with that obtained in the infinitesimal displacement case with the crucial exception that B is a linear function of the nodal displacement δ .

3. ELASTO-VISCOPLASTIC ANALYSIS OF SOLIDS

3.1 Viscoplastic Constitutive Law for Adhesive Material

Viscoplastic behaviour is governed by the scalar yield function of the form

$$F = \bar{F}(\sigma_{ij}, \epsilon_{ij}^{vp}, k) - \sigma_y(k) = 0 \quad (33)$$

in which σ_y is the uniaxial or effective yield stress, ϵ_{ij}^{vp} is the viscoplastic strain, k is a history-dependant hardening parameter and the value of $F < 0$ implies an elastic state. The viscoplastic strain rate is expressed in its general form as a function of the current stress according to

$$\dot{\epsilon}_{ij}^{vp} = f(\sigma_{ij}) \quad (34)$$

The specific form of the above equation proposed by Perzyna¹⁷ is employed as

$$\dot{\epsilon}_{ij}^{vp} = \gamma \langle \phi(F) \rangle \frac{\partial Q(\sigma_{ij})}{\partial \sigma_{ij}} \quad (35)$$

in which γ is the fluidity parameter controlling the plastic rate, $\phi(F)$ is a positive monotonic increasing flow function, and the notation $\langle \rangle$ implies that the viscoplastic straining occurs only for values of $\phi(F) > 0$. The scalar quantity Q can be interpreted as a plastic potential and for associated viscoplasticity $Q = F$, where F is the yield function. Several choices have been recommended for the function ϕ , but the two most common forms as per Owen and Hinton¹⁸ are

$$\phi(F) = e^{M(\bar{F} - \sigma_y)/\sigma_y} - 1 \quad (36)$$

and

$$\phi(F) = \left[(\bar{F} - \sigma_y)/\sigma_y \right]^N \quad (37)$$

in which M and N are constants. The fluidity parameter γ and the function $\phi(F)$ are determined experimentally. Finally, the total rate of stress medium can be expressed as

$$\dot{\sigma}_{ij} = C_{ijkl} (\dot{\epsilon}_{kl} - \dot{\epsilon}_{kl}^{vp}) \quad (38)$$

where C_{ijkl} is the usual constitutive tensor for elastic materials.

As the material considered is isotropic, the yield function F is rewritten as

$$F(\sigma_{ij}) = F(\sigma_m, J_2', J_3') - \sigma_y(k) \quad (39)$$

In the similar way Q is also defined, in which σ_m is the mean stress and J_2' and J_3' are the second and the third invariants of the deviatoric stresses, (S_{ij}) , respectively.

3.2 Yield Criterion for Adhesive Material

Modified von Mises yield criterion suggested by Gali¹⁹, *et al.* is given by

$$k_a \tau_{oct} + k_v \sigma_m = 1 \quad (40)$$

$$\tau_{oct} = \frac{1}{3} \left[(\sigma_1 - \sigma_2)^2 + (\sigma_2 - \sigma_3)^2 + (\sigma_3 - \sigma_1)^2 \right]^{1/2} \quad (41)$$

$$\sigma_m = \frac{1}{3} [\sigma_1 + \sigma_2 + \sigma_3] \quad (42)$$

where k_a , k_b are the material constants responsible for the yield due to the distortional and isotropic stress components, respectively. Equation (41) can be written in terms of stress invariants as

$$F = C_s (J_2)^{1/2} + C_v J_1 - \sigma_y \quad (43)$$

where

$$C_s = \frac{\sqrt{3}(1+\lambda)}{2\lambda}, \quad C_v = \frac{(\lambda-1)}{2\lambda}, \quad \lambda = \frac{\sigma_c}{\sigma_t}$$

and J_1 is the first invariant of the general stress and λ is the ratio between compressive and tensile yield stress. The effective strain is given by

$$e = C_s \frac{1}{1+\nu} (\gamma_2')^2 + C_v \frac{1}{1-2\nu} \gamma_1' \quad (44)$$

where ν is the Poisson's ratio, γ_2' is the second invariant of deviatoric strain tensor and γ_1' is the first invariant of the general strain tensor.

In this analysis, the nonlinear stress-strain behaviour of the adhesive material is represented by Ramberg-Osgood equation as well as by a bilinear hardening curve. Ramberg-Osgood curve was obtained by the least square technique⁵.

4. FINITE-ELEMENT MODELLING

The finite-element analysis is based on large displacement and large rotation but small strain assumption, which is physically appropriate for single

lap joint of eccentric loading. Explicit form of total Lagrangian approach is adopted. On the part of establishing equilibrium equations, incremental formulation is implemented in which static and transient values are updated incrementally corresponding to the successive time steps (or load steps) to trace out the complete solution path. In this solution, it is important that the governing finite-element equations are satisfied at each time step to sufficient accuracy, otherwise the solution errors can be significantly accumulated and which can lead to the solution instabilities. These aspects as well as incremental time-stepping algorithm for the elasto-viscoplastic problem have already been covered⁴.

Displacement convergence criterion is used with the tolerance limit in the order of 10^{-2} to 10^{-6} , depending upon the desired accuracy. In the viscoplastic algorithm, convergence of the numerical process to the steady state is monitored by comparing the values of the viscoplastic strain rate determined during each time step. The steady state conditions are deemed to be achieved at the end of time step n , if

$$\left| \frac{\Delta t_{n+1} \sum \frac{All}{G.P} \dot{\epsilon}_{n+1}^{vp}}{\Delta t_1 \sum \frac{All}{G.P} \dot{\epsilon}_1^{vp}} \right| \leq TOLER \quad (45)$$

where $\dot{\epsilon}_{n+1}^{vp}$ is the effective strain rate at the end of the n^{th} iteration. TOLER is the specified tolerance.

A single lap joint of adhesive thickness 0.3 mm is modelled using 3-D 20-noded isoparametric elements with $3 \times 3 \times 3$ Gaussian integration scheme. Overall dimensions and the boundary conditions

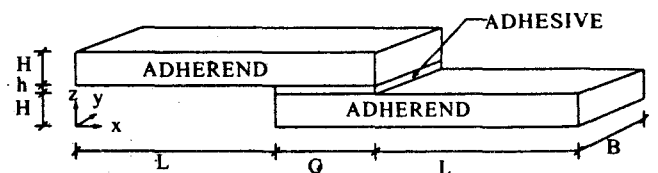


Figure 2. Single lap joint model with dimensions ($L=32.0$ mm, $C = 16.0$ mm, $H = 1.6$ mm, $h = 0.30$ mm, $B = 1.0$ mm, 4.0 mm, 8.0 mm, 12.0 mm, 16.0 mm, 24.0 mm, and 32.0 mm.

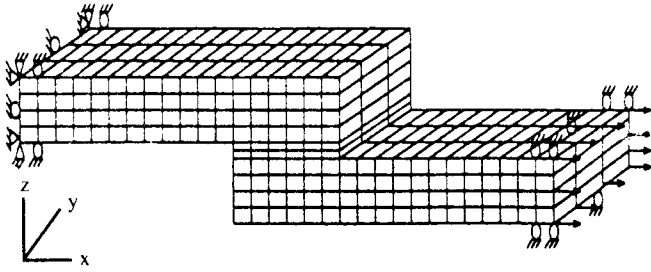


Figure 3. Typical finite-element mesh with boundary conditions

of the joint are given in Figs 2 and 3. The finite-element model has 560 elements and 3453 nodes. The properties of the materials are listed in the Table 1. A single lap joint is analysed for four different cases, viz., linear-elastic, elastic solution with geometric nonlinearity, elasto-viscoplastic and elasto-viscoplastic with geometric nonlinearity. For linear-elastic and elasto-viscoplastic analyses the load is applied in one increment whereas for geometric nonlinearity, load is applied in ten increments of equal load factor. The initial yield stress for adhesive and adherend are given larger values so as to remain in elastic region for linear-elastic and elastic solution with geometric nonlinearity. Viscoplastic analyses are performed by adopting the explicit scheme with the initial time step length equal to 0.1 and time step increment is 1.5. Explicit time scheme is being used instead of implicit time scheme since Pandey⁵ has shown that the execution time per iteration for implicit scheme is more and the economical and

Table 1. Material properties of adhesive and adherend

Items	Adherend (steel)	Adhesive (FM-73)
E	21000.0 MPa	2210.0 MPa
σ_y	5000.0 MPa	40.0 MPa
γ	-	$4.495 \times 10^{-3}/s$
$\phi(F)$	-	$\frac{(F - F_0)^N}{F_0}$
N	-	1.426
λ	-	1.400

accurate solutions can be obtained by explicit time integration scheme. 3-D viscoplastic analyses, is performed to look at the stresses in adhesive layer and three different set of the results are presented, viz.,

- Influence of geometric nonlinearity: Comparison of stress distribution in the adhesive layer for linear-elastic, elastic solution with geometric nonlinearity, elasto-viscoplastic solution and elasto-plastic solution with the geometric nonlinear effect.
- Elasto-viscoplastic analysis: Peel and shear stresses at different time from linear to steady state when the adhesive material is viscoplastic.
- 3-D zones in a single lap joint: Identification of 3-D zones in the adhesive layer on comparison with the 2-D plane strain results of Pandey^{5,8}, *et al*.

5. RESULTS & DISCUSSION

5.1 Influence of Geometric Nonlinearity in Single Lap Joint

For linear-elastic and elasto-viscoplastic analyses, the load is applied in one increment whereas for geometric nonlinearity, the load is applied in ten increments of equal load factor. The initial yield stress for adhesive and adherend are given larger values so as to remain in elastic region for linear-elastic and elastic solutions with geometric nonlinearity. Deformation of a single lap joint under the effect of geometric nonlinearity can be seen in Fig. 4. Results of peel and shear stresses for various analyses are shown in the Figs 5 and 6 and the following comparisons are made based on the results:

- Maximum peel stress occurs at the end of the overlap length for all cases.
- Maximum peel stress decreases for the analyses of linear-elastic, elastic with geometric nonlinearity, elasto-viscoplastic, and elasto-viscoplastic with geometric nonlinearity.
- Geometric nonlinear analysis reduces the maximum peel and shear stresses at the end portion of overlap for both elastic and elasto-viscoplastic solutions.

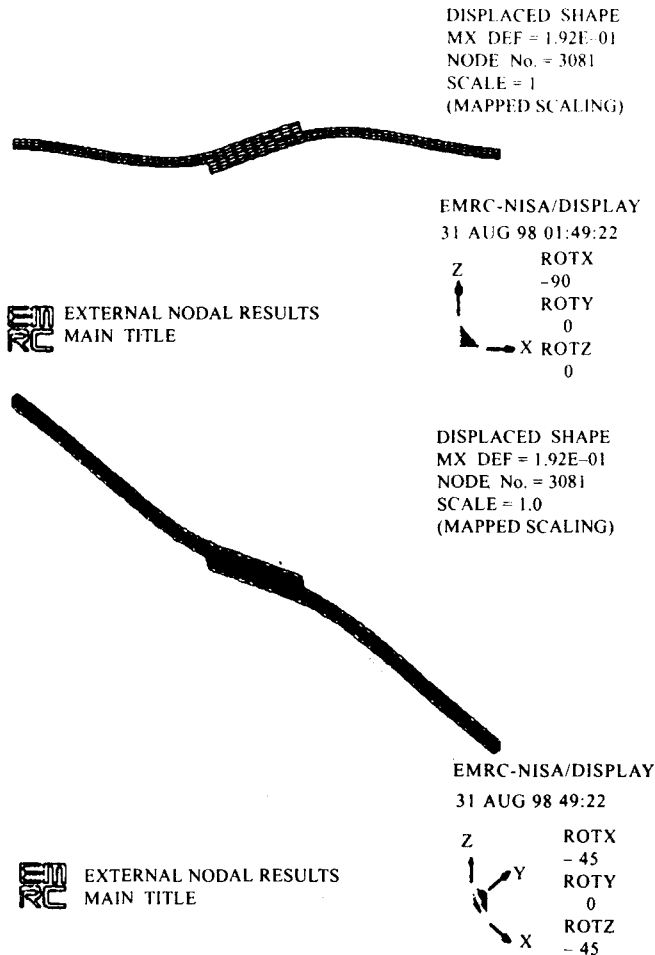
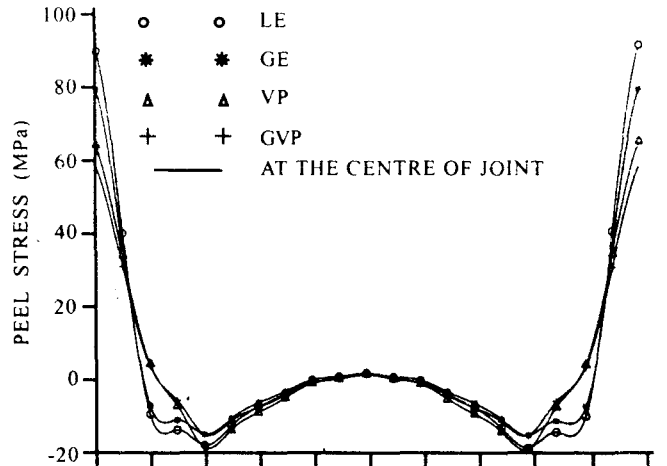
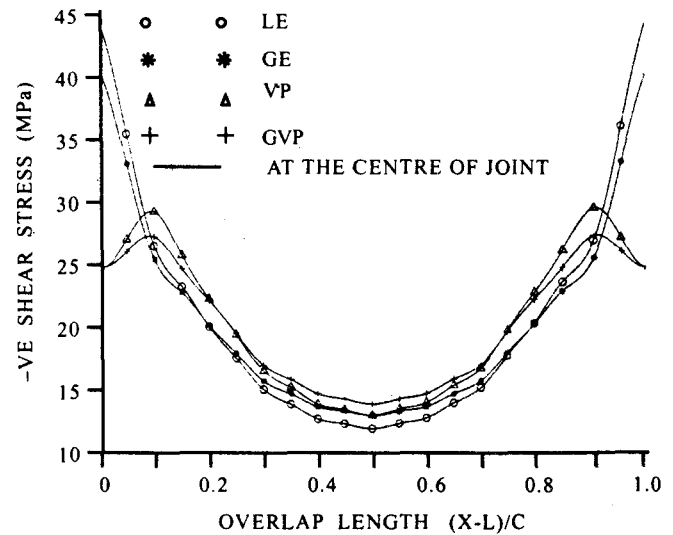


Figure 4. Deformation of a single lap joint

- In linear elastic analysis with geometric nonlinearity, peak peel and shear stresses are around 80 per cent and 90 per cent, respectively of the maximum values obtained without considering geometric nonlinearity.
- Also in elasto-viscoplastic solution with geometric nonlinearity, peak peel and shear stresses are around 90 per cent and 93 per cent, respectively of the maximum values obtained without considering geometric nonlinearity.
- From the above two observations it can be deduced that the reduction in peak peel stress is more pronounced than reduction in peak shear stress due to the effect of geometric nonlinearity for both the linear-elastic and elasto-viscoplastic analyses.
- All these observations are in good agreement with the 2-D results of Pandey⁵.



(a)

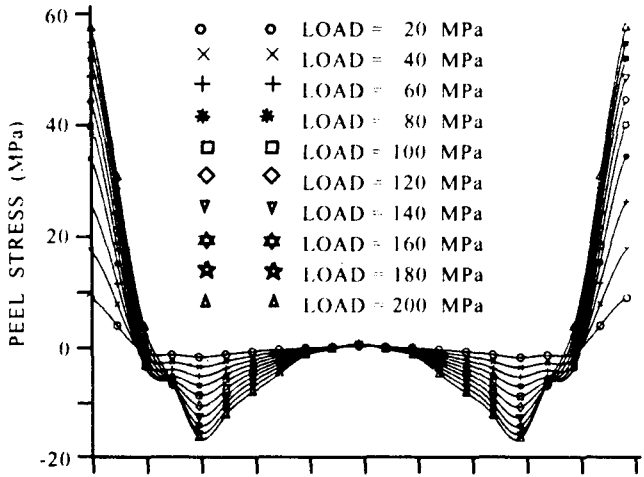


(b)

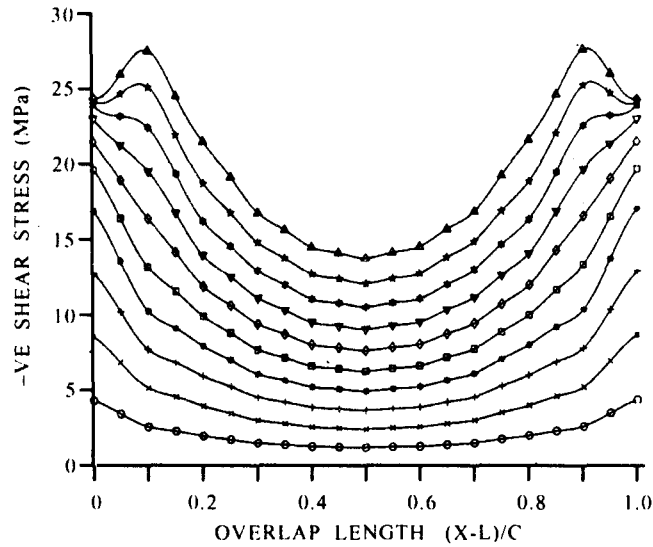
Figure 5. Peel stress and shear stress distributions for different types of analyses at $y = 0.5$ and $z = 1.75$ (for $B = 1.0$ mm; LE-linear elastic solution; GE-geometric nonlinear elastic solution; VP-viscoplastic solution; GVP-geometric nonlinear viscoplastic solution).

5.2 Elasto-viscoplastic Analysis

Peel and shear stress distributions at the middle layer of the adhesive in the central section of the joint is shown in Fig. 7. The lap joint is subjected to the tensile load of 200 MPa in one increment and the adhesive material is given elasto-viscoplastic properties. Stresses are redistributed in the adhesive layer till it reaches the steady state solution. The stress curves show the stress variation at different time values, starting from time equal to zero, which is the linear elastic solution. The steady state solution



(a)

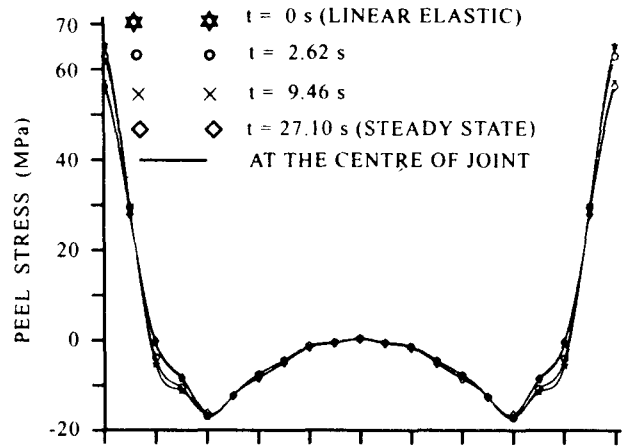


(b)

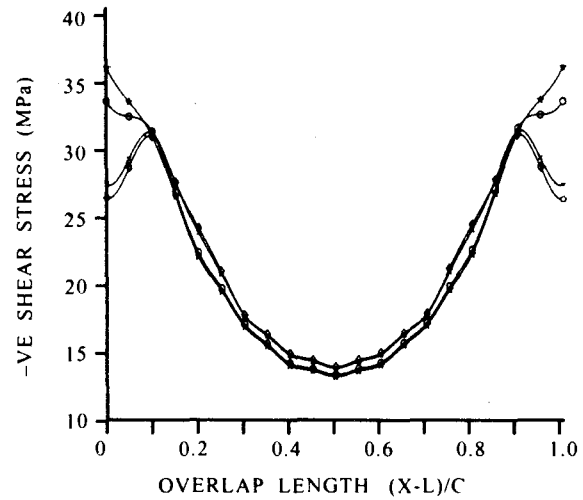
Figure 6. Peel and shear stress distributions for different load increments.

which corresponds to elasto-plastic analysis was reached over the period of 27.1 s and it took 66 iterations. From the plots, following points can be deduced:

- Distribution pattern of peel and shear stresses is the same for different time values.
- Peel stress variation is pronounced at the overlap edges than at the central overlap length.
- Peak peel stress always occurs at the end of overlap length.
- Peak peel stress decreases with the time and peak steady state values are 85 per cent of the linear elastic solution.



(a)



(b)

Figure 7. Peel and shear stress distributions with time at $y = 8.0$ mm and $z = 1.75$ mm (for $B = 16.0$ mm).

- Peak shear stress decreases with the increase in period and there is shift in the location of peak stress towards the middle region of overlap length indicating the sensitivity of viscoplastic material with time.
- Steady state peak shear stress is around 72 per cent of the linear stress value.

5.3 Identification of 2-D & 3-D Zones in a Single Lap Joint

Three-dimensional zones in a single lap joint are identified from the zones of plane strain behaviour (i.e. 2-D zone) by comparing the 3-D results with the 2-D results of Pandey^{5,8}, *et al.* Peel and shear stresses were plotted along the width of the joint at different locations of the overlap length.

Both the overlap length and the width were made normalised so that the results of different width could be plotted in one graph. The plane strain value (Pandey⁵, *et al.*) was kept the same throughout the unit width of the joint. This value was picked

and plotted as a straight line on the graph of 3-D results. Now this will enable one to compare the values at various places along the width of the joint. These plots are given in Figs 8 and 9. The 3-D plots given in Figs 10 and 11 may also be

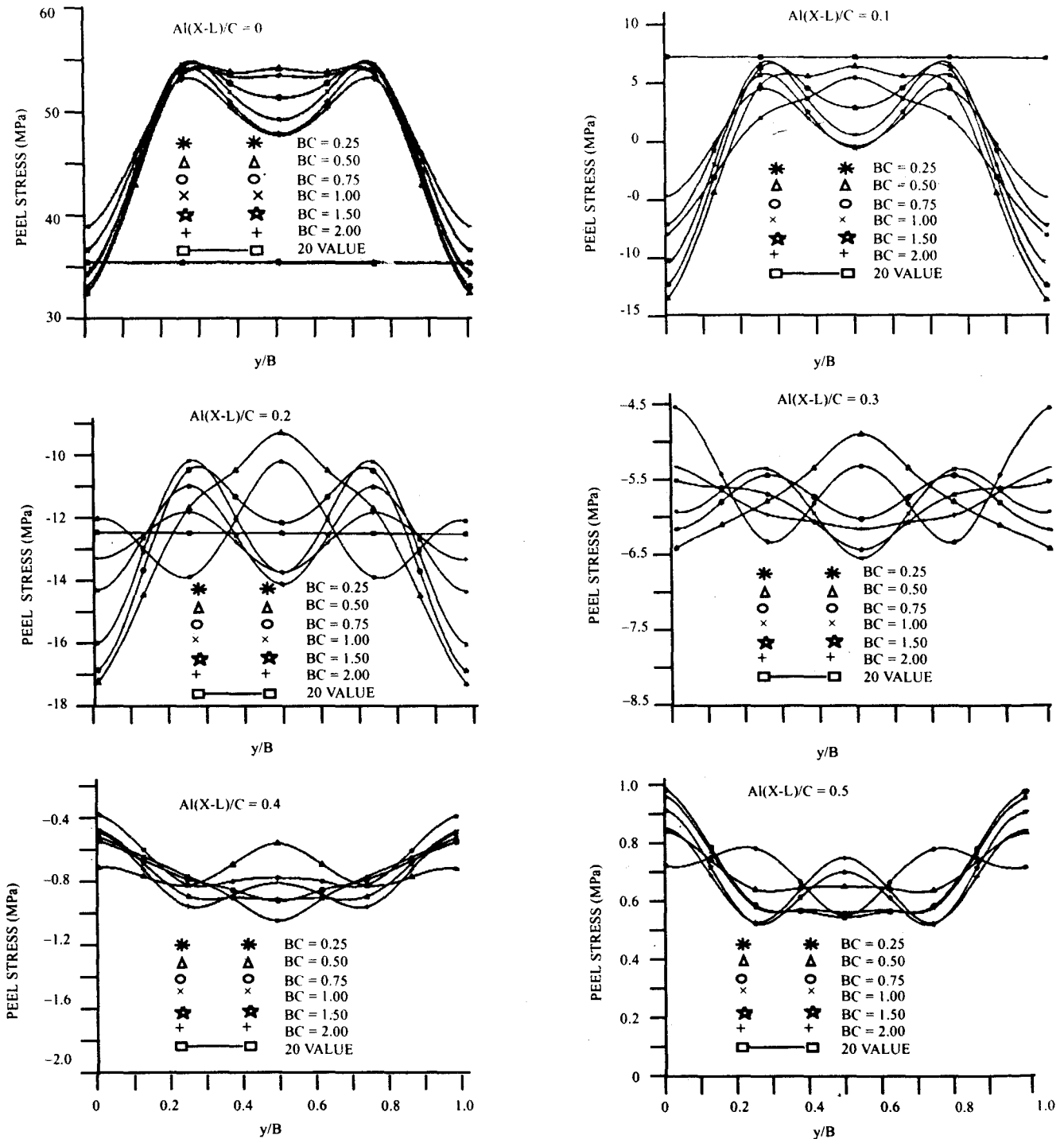


Figure 8. Peel stress distributions for various B/C ratios at (X-L)/C = 0, 0.1, 0.2, 0.3, 0.4, 0.5

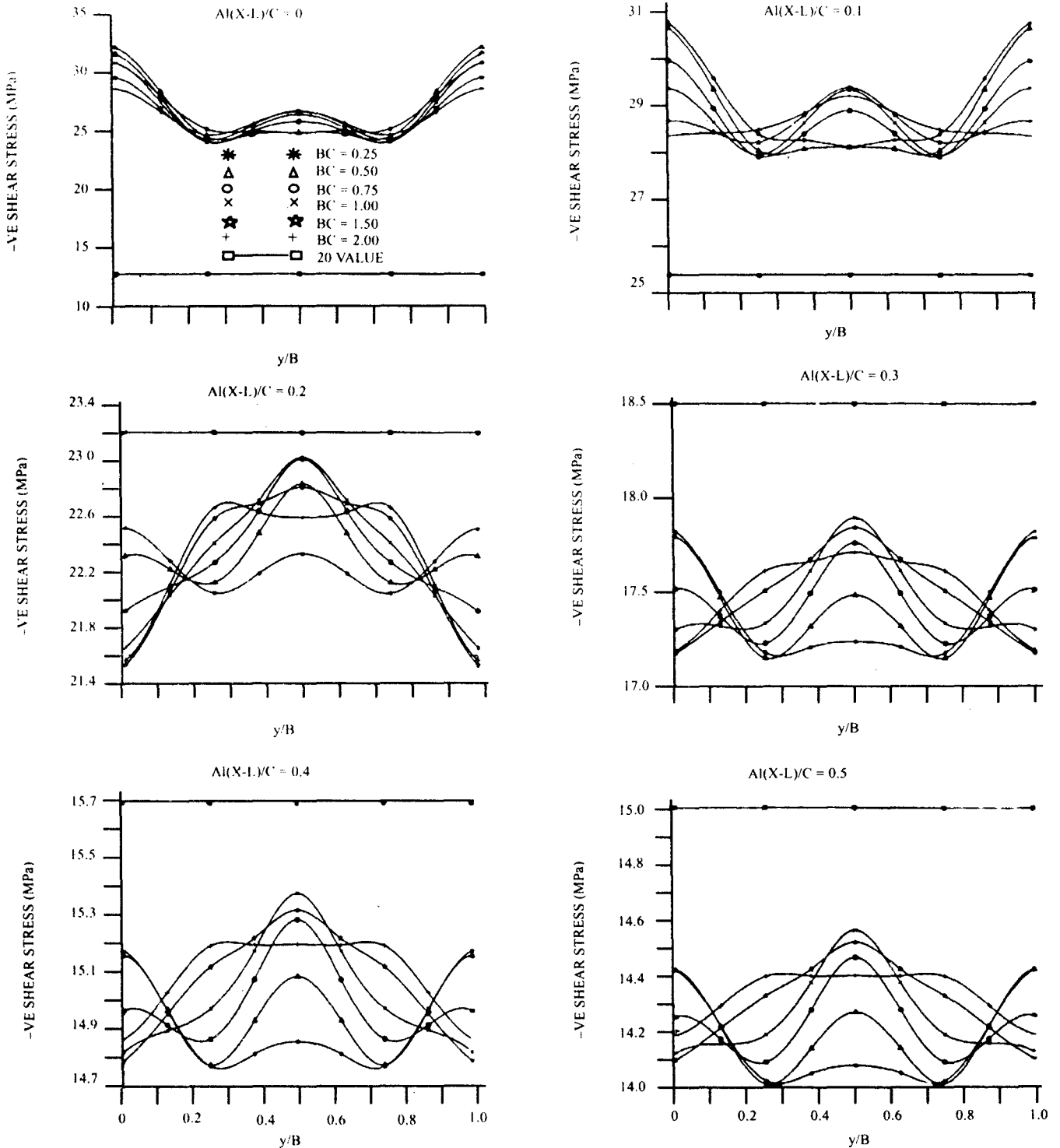


Figure 9. Shear stress distributions for various B/C ratios at (X-L)/C = 0, 0.1, 0.2, 0.3, 0.4, 0.5

referred to identify 3-D zones. The observations made from the plots are as follows:

- Behaviour at the edges: The peel stress values are close to plane strain at the edges. In particular,

the values are matching with the 2-D value for the distance of 5 per cent on the ends of lateral width for the ratios B/C=0.25, 0.5, 0.75. In the other places, 3-D effect is more pronounced.

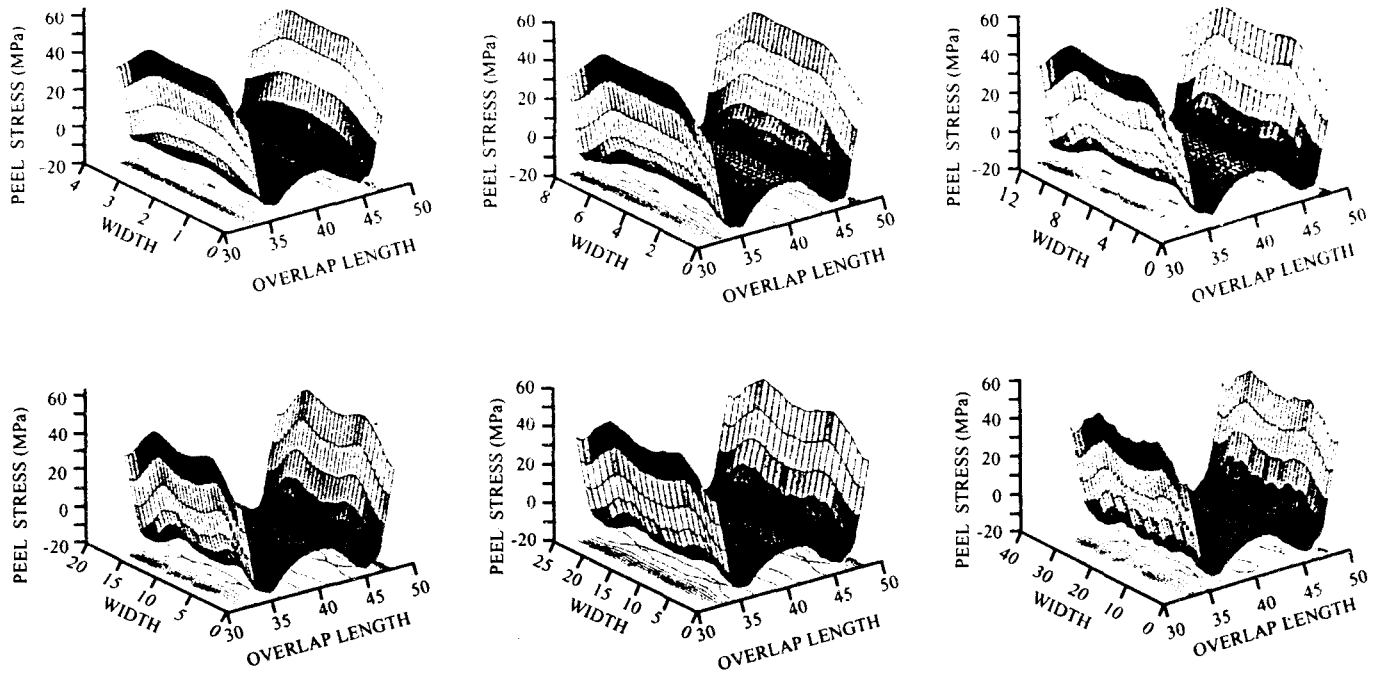


Figure 10. Three-dimensional peel stress distributions for various B/C ratios: 0.25, 0.50, 0.75, 1.00, 1.50 and 2.00

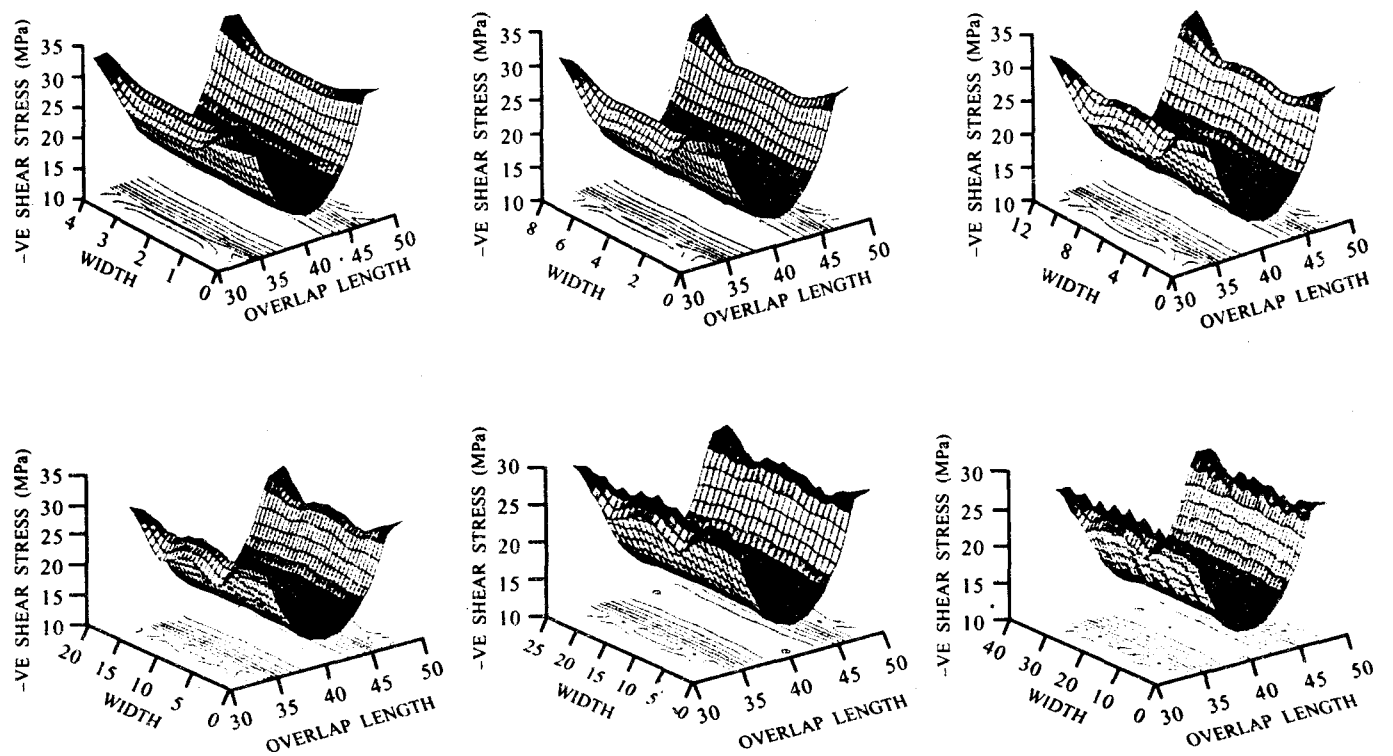


Figure 11. Three-dimensional peel stress distributions for vaious B/C ratios: 0.25, 0.50, 0.75, 1.00, 1.50 and 2.00

With regard to shear stress, the behaviour is visibly 3-D for all the ratios.

- Behaviour at the centre: The peel and shear stresses are picked at the centre of the overlap length. Comparing with 2-D value, it is clear that the 3-D behaviour is enhanced throughout the width, but it should be noted that the magnitude is not very significant from 2-D value for both the peel and the shear stresses.
- Behaviour at other places: The peel distributions at other places also show 3-D regions clearly from the plane strain locations. But on the part of shear stress, plane strain value is matching with the stresses at the centre of the lateral width and at the overlap locations 10–20 per cent on either side of the centre. It is not the same case at 30-40 percent of the lap length and 3-D effect is more pronounced for the full width. Shear stresses too show the variations but the differences on the magnitude are in the range of 2 MPa to 6 MPa.

6. CONCLUSIONS

Three-dimensional geometric nonlinear finite-element analysis of adhesively bonded single lap joint, considering viscoplasticity, is presented. Total Lagrangian method is formulated to consider the geometric nonlinearity in a single lap joint due to finite rotation of the joint. The stress-strain of the adhesive material is modelled by the Ramberg-Osgood equation. Modified von Mises criterion is employed for the adhesive material. Viscoplastic analysis together with geometric nonlinearity gives the reduced stresses at the end of overlap than the elastic solution. From the observations made on the identification of 3-D zones, it is concluded that 3-D analysis shows significantly different distribution of stresses from the plane strain analysis away from the central region. Hence, the need for 3-D analysis is recommended for behavioural study and joint design.

REFERENCES

1. Carpenter, W.C. Finite element analysis of bonded connections. *Int. J. Num. Engg.*, 1973; **6**(3), 450-51.
2. Dattaguru, B.; Everett, R.A.; Whitcomb, J.D. & Johnson, W.S. Geometrically nonlinear analysis of adhesively bonded lap joints. *J. Engg. Mater. Tech.*, 1984, 106:59.
3. Harris, J.A. & Adams, R.D. Strength prediction of bonded single lap joints by nonlinear finite element methods. *Int. J. Adhesion Adhesives*, 1984, **4**(2), 65-78.
4. Narasimhan, S. Three dimensional viscoplastic and geometrically nonlinear finite element analysis of adhesively bonded joints. Indian Institute of Science, Bangalore, 1998. MSc Thesis.
5. Pandey, P.C.; Shakaragouda, H. & Singh, Arbind Kr. Nonlinear analysis of adhesively bonded lap joints considering viscoplasticity in adhesives. *Computers Structures*, 1999, **70**, 387-13.
6. Pandey, P.C.; Narasimhan, S. & Maruthi Pavan, P.V.R. Three dimensional viscoplastic analysis of adhesively bonded lap joint. *In Proceedings of 8th National Seminar on Aerospace Structures (NASAS-8) 1998*, pp. 135-42.
7. Pandey, P.C. & Narasimhan, S. Three-dimensional viscoplastic and geometrically nonlinear finite element analysis of adhesively bonded single lap joint 1999. Project Report Dept of Civil Engg., Indian Institute of Science, Bangalore. AR&DB Report No. Aero/RD-134/100/10/96-97/924,
8. Pandey, P.C. & Narasimhan, S. Three-dimensional nonlinear analysis of adhesively bonded lap joints considering viscoplasticity in adhesives. *Computers Structures*, 2001, **79**, 769-83.
9. Pickett, A.K. & Hollaway, L. The analysis of elastic adhesive stresses in bonded lap joints in FRP structures. *Composite Structures*, 1985, **3**, 55-79.
10. Roy, S. & Reddy, J.N. Nonlinear analysis of adhesively bonded joints. *Int. J. Nonlinear Mech.*, 1988, **23** (2), 97-112.
11. Roy, S. & Reddy, J.N. Finite element models of viscoelasticity and diffusion in adhesively

- bonded joints. *Int. J. Num. Meth. Engg.*, 1988, **26**, 2531-546.
12. Tsai, M.Y. & Morton, J. Three-dimensional deformations in a single lap joint. *J. Strain Analysis*, 1994, **29**(1), 137-45.
 13. Zienkiewicz, O.C. The finite-element method in engineering science. Ed. 4. McGraw-Hill, 1991.
 14. Hill, R. On constitutive inequalities for simple materials-I. *J. Mech. Phys. Solids*, 1968, **16**, 229-42.
 15. Zienkiewicz, O.C. & Nayak, G.C. General approach to problems of plasticity and large deformation using isoparametric element. *In 3rd Conf. Matrix Methods in Structural Mechanics*. 1973. Wright-Patterson Air Force Base, Ohio. pp. 881-928.
 16. Schrefler, B.A.; Odorizzi, S. & Wood, R.D. A total Lagrangian geometrically nonlinear analysis of combined beam and cable curves. *Computers Structures*, 1983, **17** (1), 115-27.
 17. Perzyna, P. Fundamental problems in viscoplasticity. *In Recent advances in applied mechanics*, Vol. 9. New York, Academic Press, 1966. pp. 243-377.
 18. Owen, D.R.J. & Hinton, E. Finite elements in plasticity: Theory and practice. Swansea Pineridge Press, 1980.
 19. Gali, S.; Dilev, G. & Ishai, O. An effective stress/strain concept in the mathematical characterisation of structural adhesive bonding. *Int. J. Adhesion Adhesives*, 1981, **1**, 135-40.

Contributor



Mr S Narasimhan obtained his MSc (Structural Engineering) from the Indian Institute of Science (IISc), Bangalore, in 1998. He worked as Project Engineer in Quality Engineering Software Technologies Ltd, where he was involved in finite-element analysis and design of gas turbine machines for GE-powersystems, USA. He has been doing his PhD since 1999. He has published three papers in national/international journals.